

Mean Wind Pressure Distribution on Composite Plan Tall Building

Suresh Nagar¹&Rahul Bansiwala*²
^{1,2}Rajasthan Technical University, Kota, Rajasthan (India)

Abstract:

The present study demonstrates the pressure distribution on various faces of a composite plan shaped tall building model. The building model comprises of a plus shape structure up to a height of 300mm and a square shape for the next 300mm making the total height of the structure 600mm. The length scale is taken as 1:300. Analytical study is done in present work using Computational Fluid Dynamics (CFD) package of Ansys CFX. Based on study pressure contours at all faces of building model is plotted and discussed for wind incidence angles 0° and 90° . It is observed that in both cases pressures on the opposite faces of the axis of symmetry were almost identical. This study also shows the systematic variation of pressures across all faces with the help of pressure contours. Presence of re-entrant corners affects the pressure at connected faces. Effect of limb size is also observed on pressure distribution on faces.

Keywords

CFD, Flow Separation, Pressure Coefficients, Drag Coefficient, Fluid Domain

1. Introduction

Wind engineering is defined as the rational treatment of natural wind and manmade structures in the atmospheric boundary layer. With increasing population and decreasing available land the requirement of high rise buildings is at its peak in the current scenario. The building design codes of India and other countries provides pressure variation and force coefficients for conventional plan shapes only and not any for the irregular plan shapes which are more preferred these days due to the increased aesthetic value and higher available land use capacity. Wind tunnel and CFD studies are carried out to check the responses on irregular plan shapes acting due to wind forces. Kareem (1992) presented a study focusing on dynamic response of high rise buildings of generic building shapes of different aspect ratios. Kumar and Swami(2010) deliberated

the details of wind effects on tall building frames using the Gust Effectiveness Factor method. Raju et al (2013) modeled a 3B+G+40 storey RCC high rise building for wind loads and seismic loads as per the IS code of practice. Tse et al(2017) enumerated the results of a series wind tunnel studies done on nine building models of different heights and passage widths under twisted wind flows. Ahlawat and Ahuja(2015) carried out an experimental study using a Wind tunnel on a 'T' plan shape building model to evaluate base shear, overturning moment and torsional moment both in isolated as well as interference conditions. Kheyari and Dalui(2015) proposed a case study of interference effect due to a interfering building model of height 100 mm on a high rise building model of height 500 mm using CFD package.

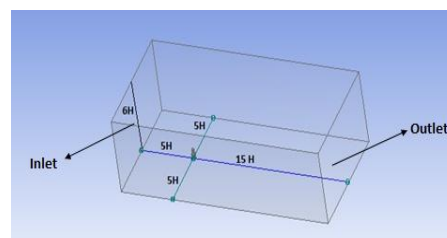


Figure 1. Domain used in study

Paul and Dalui(2016) examined in detail the distribution of mean pressure at various faces of a Z plan shaped building model due to wind loads using the analytical technique of CFD. Kar and Dalui(2016) investigated the wind interference effect on the faces of an octagonal shaped tall building due to interference of 3 square shape buildings closely spaced and of same height. Lohade and Kulkarni(2013) enumerated the results of the analytical study of wind effects on tall building models of different geometric configurations all having same plan area. Verma et al(2013) discussed the results of a study done on square plan shape tall building model tested in a closed circuit wind tunnel under boundary layer flow. Bharat and Ahmed(2012) discussed the findings on a study done to monitor the effect of tall building on wind flows around the tall building.

Bhattacharyya et al.(2014) correlated results of experimental and analytical study done to demonstrate pressure distribution on various faces of E plan shape tall building.

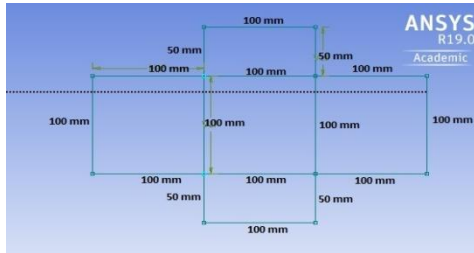


Figure 2. Plan of building model

Sanayei et al. (2003) investigated the effects of increased wind loading due to change in climate on a fifty storied building in the Boston metropolitan area.

Table 1. Comparison of C_{pe} to validate CFD

As per	$\frac{h}{w}$	C_{pe} for faces			
		A	B	C	D
Ansyes CFX	$\frac{h}{w}=5$	+0.81	-0.29	-0.78	-0.78
I.S:875 (Part 3) 1987	$\frac{3}{2} < \frac{h}{w} < 6$	+0.80	-0.25	-0.80	-0.80

2. Mean Wind Speed Profiles

Velocity of wind is considered 0 at the exact ground surface and is found to be increasing as the height from the earth's surface increases. This kind of wind velocity profile can be presented by two models namely, logarithmic law and the power law.

2.1. Logarithmic Law: $\frac{Vz}{V^*} = \frac{1}{k} \log_e \frac{z}{z_0}$

where k is Von Karman's constant = 0.41, z is the height above ground, z_0 is the ground roughness parameter V^* is friction viscosity = $\sqrt{\frac{\tau}{\rho}}$, τ is the skin frictional force on the wall and ρ is the air density.

2.2. Power Law: $\frac{V}{V_0} = \left(\frac{z}{z_0}\right)^\alpha$

where V is the velocity of wind at a height z , V_0 is the wind speed at a reference height, z is the height where wind velocity need to be calculated, z_0 is a reference height, α is known as the power law coefficient which depends on the terrain on which building is placed. Out of the above two methods

Power law is widely used by researchers as it easy to compare with the mean wind velocity profile. In this study also power law is used to generate atmospheric boundary layer.

3. Computational Fluid Dynamics

Computational fluid dynamics (CFD) is a computer simulation tool which evaluates the interaction of wind and structures numerically offering a reliable alternative to traditional wind tunnel test. CFD is based on the Naiver Stokes equation which describes a relation between velocity, pressure, temperature and density of a moving fluid. Here numerical study is carried out using ANSYS CFX software, with $k-\epsilon$ turbulence modeling so as to resemble maximum with the experimental evaluation. The standard $k-\epsilon$ model comprise of two transport equations, one for k (turbulence kinetic energy) and the other one for calculation of ϵ (energy dissipation rate).

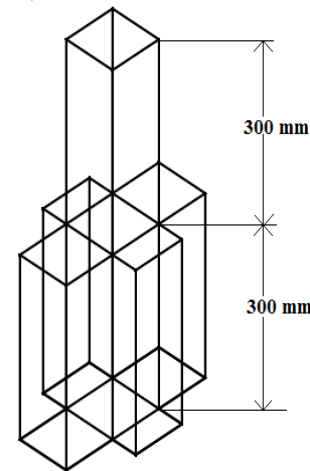


Figure 3. Elevation of the building model

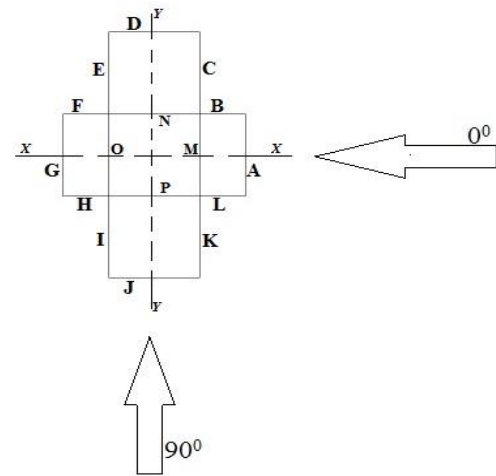


Figure 4. Different faces with wind angles of building model

The values of k and ϵ are used to define the velocity scale and the length scale at any given time in the fluid flow field in terms of the following equations:

Velocity scale, $U = k^{1/2}$, Length scale, $l = \frac{k^{3/2}}{\epsilon}$, Where, k is the turbulence kinetic energy (TKE), ϵ is the rate of dissipation of kinetic energy. Franke et al. (2007) suggested that inlet, outlet, two side face and top clearances of the domain be 5H, 15H, 5H and 6H respectively from the edges of the building where H is the height of the building shown in fig1 is adopted in this study. The domain is meshed with a combination of tetrahedron and hexagonal elements. The building surface is meshed with finer hexagonal meshing which is obtained by inflation which helps

in generating uniform flow around the building and increases the accuracy of calculations.

4. Validation of CFD

Before starting the numerical study of the current model, validation of CFD package is done comparing with IS 875(Part 3): 2015. For this a square plan shaped model of dimension 100 x 100 mm, the height of the model being 500 mm which means aspect ratio 1: 5 is analyzed in the domain size discussed earlier using $k - \epsilon$ turbulence model with Ansys CFX package under uniform flow.

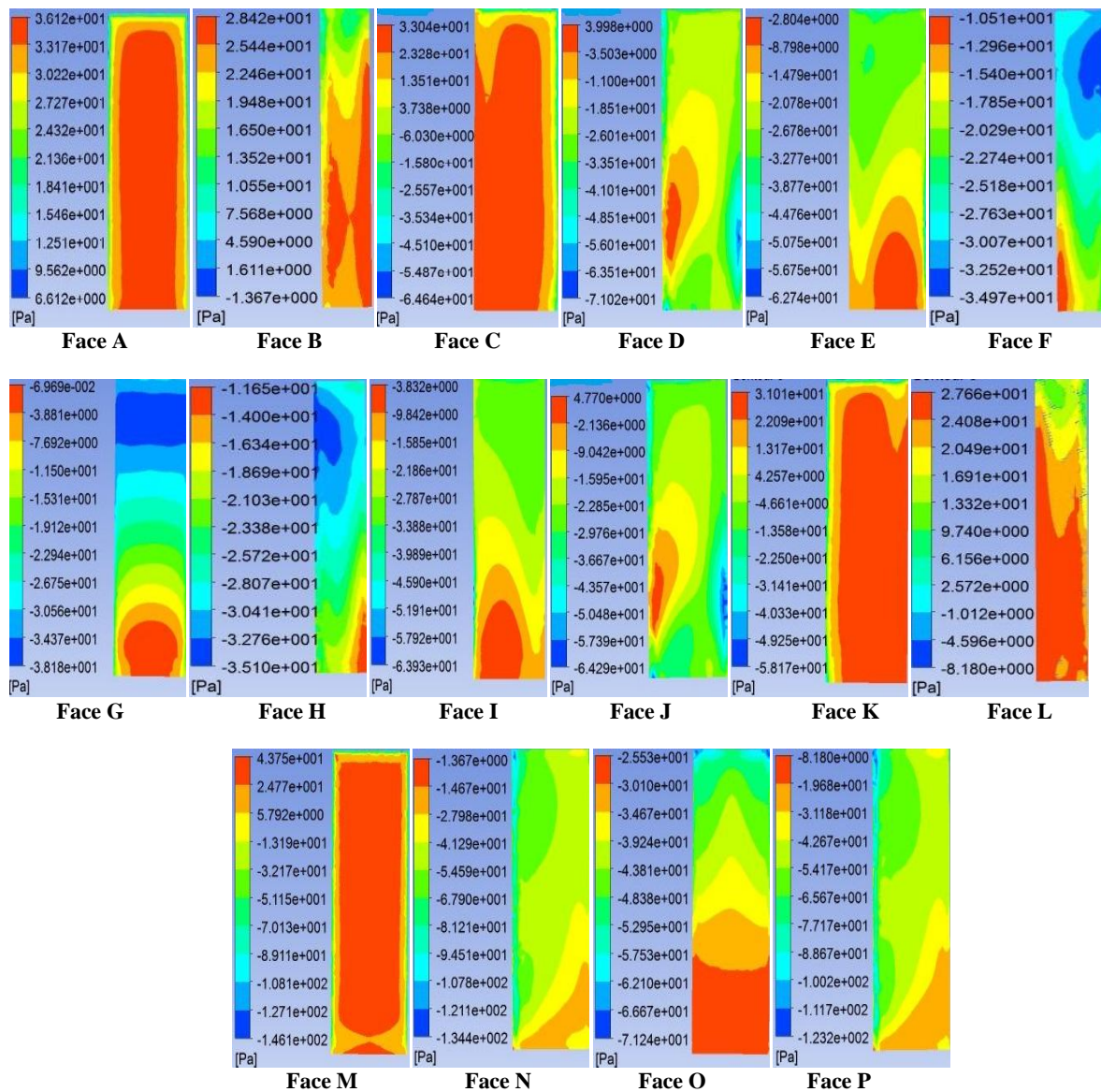


Figure 5. Pressure distribution for wind angle 0°

Wind flow velocity is generated using power law at the inlet. The average value of pressures given by Ansys CFX for all four faces are calculated and compared with Indian standard code, IS 875(Part 3) : 2015. For the windward sides and the side walls there is very less deviation in the results whereas a variation of 16 % can be seen for the face at the leeward side. This deviation in results may be due to generation of unsteady vortices in the wake region near the leeward side.

5. Results and Discussions

0° wind incidence angle passes through the X-X axis as shown in Fig. 4 which results in symmetry

of the pressures generated on the opposite faces separating from the axis.. Since the pressure generated on both side of the axis are symmetrical therefore only one side faces which are face B, face C, face D, face E, face F, face N are discussed in this paper with behavior of face A, face M and face G, face O which are the front and the back faces of the geometry. A similar pattern was also observed in case of 90° wind angle but in this case symmetry was observed along the Y-Y axis. In this case faces A,B,C,M,K,L are discussed with face J, face P and face D, face N being the front and back faces respectively.

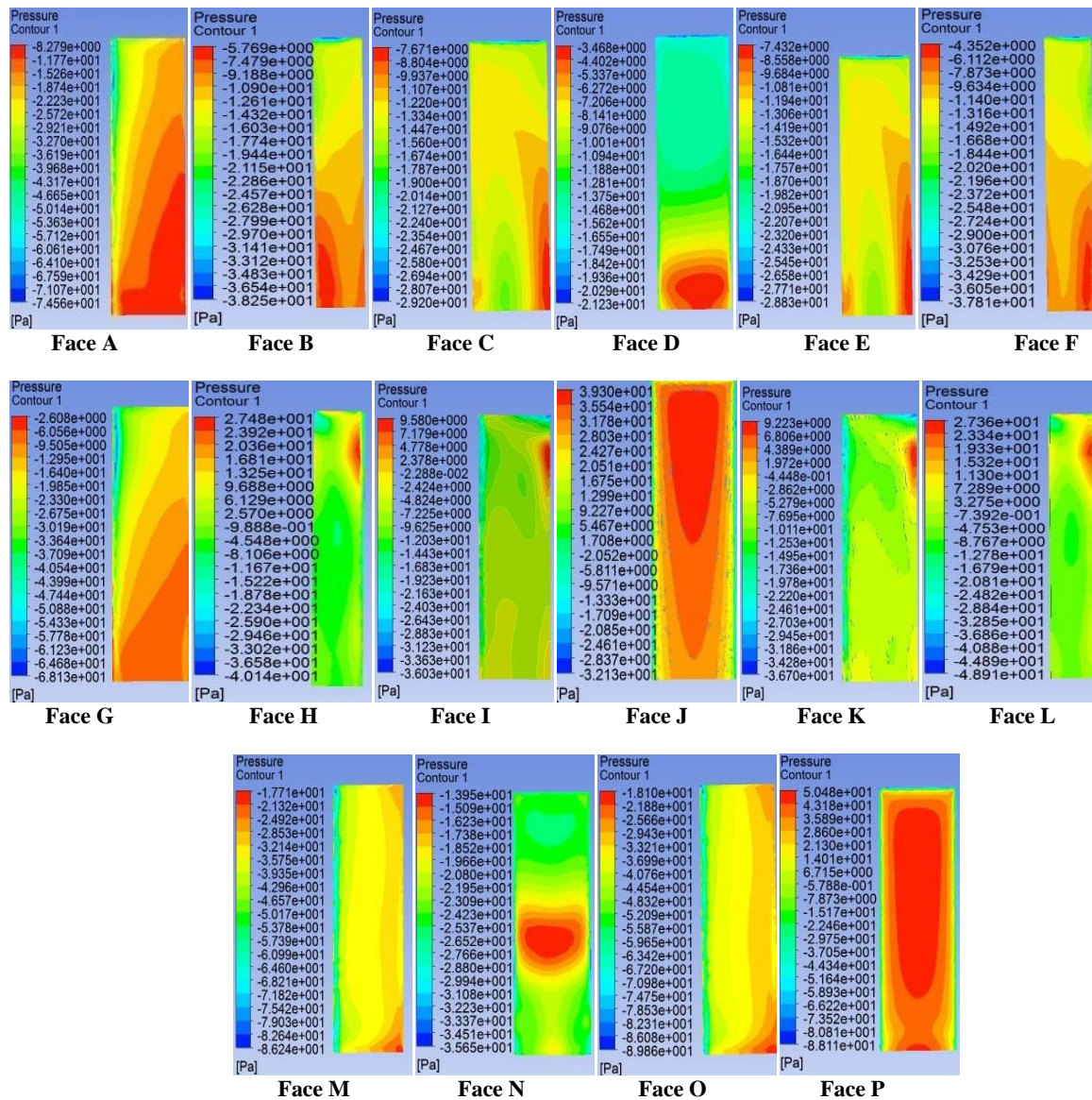


Figure 6. Pressure distribution for wind angle 90

5.1. 0° Wind incidence angle

Face A which is directly exposed to the incident wind shows a maximum pressure of 36.12 Pa concentrated around the center part of the face and moving towards the edges. The incident wind gets separated from the edges which leads very less contact of the surface with the incident wind and hence low pressure zones can be observed around the edges of face A. A very similar distribution of pressures can also be observed in case of face M but of a higher magnitude reaching a maximum pressure of 43.75 Pa. This increased pressure is in accordance with the increased wind velocity and subsequent wind forces as we move higher above the ground surface.

Side faces B and L experiences positive pressure because of increased blockage by the larger length of windward faces C and K and smaller length of these faces B and L, even though these faces are side faces parallel to faces D and J which experiences negative pressure. Face B shows positive pressures along the front edge facing towards the incident wind which rises upto a magnitude of 24.82 PA. Due to the separation of flow some part of the face does not make contact with direct wind and hence the face shows partially low pressure zones near the far end of the face. The suction pressures also suggest the formation of small eddies at the junction of face A and face C. Face C partially obstructs incident wind after getting separated from the outer edge of face A and hence both positive and negative pressures can be seen on this face. The inner side of the face shows predominantly positive pressures rises up to 33.04 Pa. This face also leads to complete separation of incident wind from the surface and hence very low or no positive pressures are seen on the leeward side faces of the building.

Face D and Face N shows mostly negative suction pressure with a very little positive of 3.99 Pa on a very small part of face D. Pressures in the direction of incident wind along X-X axis are continuously found to be decreasing and getting more and more negative. Eddies are generated along both faces D and N which are responsible for suction pressures as these faces are in no direct contact with incident wind.

Face E on the leeward side of the building is predominantly a negative pressure face. The suction pressure is less near the ground and increase with the increase in height of the building, near the ground with low wind velocity and lesser turbulence less eddies are generated but eddy size increase with increase in height showing larger negative suction pressures on the face.

Face F on the leeward side of the building shows more negative pressures near the outer edge of the face reaching a magnitude of -34.97 Pa which goes on decreasing as we move towards the inner edge of the face. In the low pressure zone the eddies formed are found more near the edges which can be seen very clearly seen in the contour plot of the face F.

Face G and Face O being the farthest from the incident wind show very clear bands of pressure increase. The suction pressure being the lowest near the ground surface of magnitude -0.0069 Pa increases with height up to a magnitude of -38.18 Pa very close to the top edge of face G. The pressure variation in case of face O is also of similar fashion. Clear band distribution can be seen which varies from lowest of -25.53 Pa near the middle edge to a highest of -62.10 Pa near the top edge of face O.

5.2. 90° Wind incidence angle

In case of a 90° wind incidence angle face J and face P are subjected to incident wind. The pressure on both faces are maximum at the top center of the faces and the decreases as we move near the edges of both faces. The maximum pressure on face J is found to be 39.30 Pa which increases as we move higher on face P and reaches a maximum of 50.478 Pa. Pressures near the edges are found very low because of minimum interaction of wind and building surface, these edges are also responsible for flow separation and eddy generation.

Faces K and L experiences negative pressure even though these are identical to faces B and L in case of 0 degree wind incidence, because of larger length of these faces and smaller length of blocking faces H and L along wind. Face K as supposed to see positive pressures show negative suction pressures because of the change in wind direction. Because of larger area of face K the flow separates before reaching the face L, and hence all faces other than faces J and P shows positive pressures on only few locations on respective faces. Face K shows a very less positive pressure of 9.22 Pa and a maximum negative pressure of -27.03 Pa around the front edge which is also the zone of flow separation.

Face L shows a positive pressure of 27.36 Pa confined only to a small area near the outer edge of the face. This pressure is due to the little contact of surface with the outwards moving wind. Rest all parts

of the face experience negative pressures because of the eddied formed between face K and L.

Face A and M being the side faces in case of 90° wind incidence angle show negative pressures only. No direct contact of wind in this region is observed, the wind crossing these faces leads to formation of large size eddies which can also be seen in the wind flow diagram. Face A shows a maximum negative pressure of -8.279 Pa which increase manifolds to -38.27 Pa in most parts of face M.

Faces B and C becomes the leeward side faces in this case forms a low pressure zone, these low pressure areas generates forces in outward direction and may cause serviceability related issues if they are in high magnitudes. Maximum portion of faces B and C experience a suction pressure of -12.20 Pa which is higher than this near the face edges.

Face D and face N are the farthest from incident wind in case of 90° wind incidence. The pressure contours of both faces are similar to farthest faces.

6. Conclusions

The influence of a composite shaped tall building comprising of a plus shape structure for the first half and a rectangle for the next half under wind loads was evaluated under boundary layer wind flow, tested in Ansys CFX package of CFD.

The study found that pressure coefficients on both sides of the axis vary in similar fashion which can be clearly seen in the contour plots drawn. This symmetrical variation of pressures can be seen in both cases of 0° and 90° wind incidence angle.

The faces on the windward sides shows positive pressures because of direct wind incidence while faces on the leeward side show suction pressures leading to formation of vortices.

Very close to the edges of the faces on the windward side negative suction pressures can also be seen depicting the flow separation and no or very less contact with the incident wind.

Effects of limb size in along wind and across wind size also affects the pressure distributions on the identical faces for 0 degree wind incidence and 90 degree wind incidence angles.

7. References

[i] Ahlawat, R., and Ahuja, A.K., "Wind Loads on 'T' Plan Shape Tall Buildings", *Journal of Academia and Industrial Research*, 4, 1, June 2015, pp. 27-30.

[ii] Bharat, A. and Ahmed, A.S., "Effects of high rise building complex on the wind flow patterns on surrounding urban pockets", *International Journal of Engineering Research and Development*, 4, 9, November 2012, pp. 21-26.

[iii] Bhattacharyya, B., Dalui, S.K., and Ahuja, A.K., "Wind induced pressure on 'E' plan shaped tall buildings", *Jordan Journal of Civil Engineering*, 8, 2, 2014, pp. 120-134.

[iv] Franke, J., Hellsten, A., Schlünzen, H., and Carissimo, B., "Best practice guideline for the CFD simulation of flows in the urban environment", Cost Office, Brussels, May 1 2007, pp. 1-52.

[v] Kareem, A., "Dynamic response of high-rise buildings to stochastic wind loads", *Journal of Wind Engineering and Industrial Aerodynamics*, 41-44, 1992, pp. 1101-1112.

[vi] Kumar, D.B., and Swami, B.L.P., "Wind Effects on Tall Building Frames, Influence of Dynamic Parameters", *Indian Journal of Science and Technology*, 3, 5, May 2010, pp. 583-587.

[vii] Kheyari, P., and Dalui, S.K., "Estimation of wind load on a tall building under interference effects: a case study", *Jordan Journal of Civil Engineering*, 9, 1, 2015, pp. 84-101.

[viii] Kar, R., and Dalui, S.K., "Wind interference effect on an octagonal plan shaped tall building due to square plan shaped tall buildings", *International Journal of Advanced Structural Engineering*, 8, February 20 2016, pp.73-86.

[ix] Lohade, S. and Kulkarni, S., "Shape Effects of Wind Induced Response on Tall Buildings Using CFD" *International Journal of Engineering and Applied Sciences ISSN*, 3, 6, June 2016, pp. 2394-3661.

[x] Paul, R., and Dalui, S. K., "Wind effects on 'Z' plan-shaped tall building: a case study", *Int Journal of Advanced Structural Engineering*, 8, August 17 2016, pp. 319-335.

[xi] Raju, K. R., Shereef, M.I., Iyer, N. R., and Gopalakrishnan, S., "Analysis and design of RC tall building subjected to wind and earthquake loads", *In Proceedings 10th Asia-Pacific Conference on Wind Engineering*, Chennai, India, December 10-14, 2013, pp. 844-852.

[xii] Sanayei, M., Edgers, L., Alonge, J., and Kirshen, P., "Effects of increased wind loads on tall buildings" *Civil engineering practice*, 18, 2, 2003, pp. 5-16.

[xiii] Tse, K.T., Weerasuriya, A.U., Zhang, X., Li, S.W., and Kwok, K.C.S., "Effects of twisted wind flows on wind conditions in passages between buildings" *Journal of Wind Engineering & Industrial Aerodynamics*, 167, April 28 2002, pp. 87-100.

[xiv] Verma, S. K., Ahuja A.K., and Pandey, A. D., "Effects of wind incidence angle on wind pressure distribution on square plan tall buildings", *J Acad Ind Res*, 1, 12, May 2013, pp. 747-75.